A dispersion of a droplet flow on crossing wires in an air counterflow

Ondřej Hájek[1*], *Ondřej* Cejpek[1], *Milan* Malý[1], *František* Prinz[1], and *Miroslav* Jícha[1]

[1]Energy Institute, Faculty of Mechanical Engineering, Brno University of Technology, Technická 2896/2, 616 69 Brno, Czech Republic

Abstract. Liquid dispersion on a wire mesh is a phenomenon that is utilized in many industrial applications, such as rotating packed beds. It is a very simple method of liquid atomization without a need for complex nozzles. This research focuses on an elementary case of a liquid dispersion on a crossing of two wires. Experiments were carried out in a wind tunnel to elucidate the influence of counterflow air velocity on a liquid sheet and droplets. High-speed camera was used to capture the impact of droplets on the crossing. Images were then processed using MATLAB® addon PIVlab. The effect of the input parameters, including a liquid flow rate in the range of 3.8 to 12 kg/h and air flow velocity varying from 0 to 9 m/s on the angle and velocity of dispersed droplets downstream of the crossing, was investigated. Finally, a qualitative description of the dispersion was evaluated. Results show that with an increasing liquid flow rate, the droplets dispersed in a wider angle. On the other hand, the influence of the air counterflow is significant only for low liquid flow rates. The atomization rate, determined by the number of small droplets, was better for higher liquid flow rates.

1 INTRODUCTION

Liquid atomization is common in all branches of industry. For example, paint is atomized into small droplets that impact the surface and create a thin layer to create coatings, or fuel is dispersed into tiny droplets that then evaporate and burn in engines. Dispersed droplets can be used for spray cooling. Finally, there are applications where liquid is used as an absorbent, and therefore the goal is to create a large interface between gas and liquid to enhance the mass transfer rate. Sprays and droplets can be created by several approaches, such as specially designed pressure swirl atomizers [1] which create spray due to interior design, two-fluid effervescent atomizers [2] or by impinging jet atomization where atomization is achieved by the impact of two liquid jets [3].

A liquid volume can also be dispersed by an impact on the solid surface, e.g., a wire or a wire mesh. This method presents a simple way to create a droplet cone or droplets without the need for complex geometries or pure liquids because it can disperse flows with particles. Possible applications of this atomization are oil-water separation [4], the delivery of pesticides and herbicides precisely above plants [5], or rotating packed beds (RPB). An RPB is a patented device [6] to increase the rate of mass transfer by adding centrifugal acceleration. A liquid jet is introduced on the inner surface of the rotating ring. The surface is formed by wire mesh [7], metal foam [8], or other shapes [9]. The jet is dispersed after an impact on the mesh. This creates liquid ligaments and droplets that further interact with the inner layers of the packing and create an interface. To improve the mass transfer rate, it is essential to understand how the first layer affects the dispersion with a consideration of the influence of the air counterflow.

The current state of the art concerning this atomization can be divided into two directions, both of which focus primarily on the impact of a single droplet on a wire or a wire mesh. This division is based on the ratio between the diameter of the mother drop before the impact and the dimensions of the wire or the mesh eye. For example, Soto et al. [5] studied millimetre droplets that impact on a fine mesh with a distance between the fibers in the order of hundreds of micrometres. This study concludes that this type of atomization seems useful for agricultural processes because it prevents the drift of pesticides to the environment. One conclusion is also that the liquid dispersion on the wire mesh increases the surface-to-volume ratio with low-energy loads. Sun et al. [10] studied different velocities of mother droplets that impact a fine superhydrophobic wire mesh. Such a liquid dispersion depends on the Weber number (We), where two types of sprays are described under the mesh for low and high We. Low We causes a droplet to bounce off the mesh, whereas droplets with high We pierce right through the mesh. The Weber number is a dimensionless number which describes the ratio between a kinetic energy and a surface energy of the drop. The impact of relatively large droplets on a fine mesh was described for other differing input parameters, such as several layers of wire meshes in Su et al. [11] or hydrophobic mesh in Zhang et al. [12]. A hydrophobic mesh shows a dispersion angle under the

* Corresponding author: Ondrej.Hajek3@vutbr.cz

mesh that is significantly greater than that of a hydrophilic mesh. Surface wettability was also studied in [13].

The other branch of these studies deals with a droplet that falls on a single wire or on the crossing of two wires. This phenomenon was studied by Tang et al. [14]. Their study focused on different velocities of mother droplets, droplet sizes, and shapes of the impacted objects. The authors found three typical dispersion modes of the liquid: one-drop mode, two-drop mode, and for some cases they described liquid ligaments. Haim et al. [15] published similar study where the authors study the amount of liquid captured on the wire, as well as the influence of the distance between the centre of gravity of the impacting droplets and the axis of the wire.

There are also several studies that describe liquid dispersion in RPBs, e.g., Lu et al. [16] or Wang et al. [17]. Both studies are affected by another input parameter, specifically rotations of the packing.

In real applications, such as RPBs, there is one parameter which seems to influence the angle of the dispersed droplets. This factor is the air counterflow. Thus, the goal of this study is to add the missing information about the influence of such a counterflow as well as to describe behaviour of the liquid jet dispersion on the wire.

2 MATERIALS AND METHODS

2.1 Wind tunnel

The whole experiment was carried out in an air tunnel described in Cejpek [18]. The test section of the tunnel was placed in the vertical position, so the gravitational acceleration is in the opposite direction to the air flow (Figure 1).

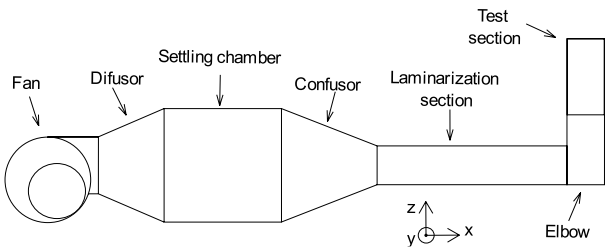

Fig. 1. Schematic layout of the wind tunnel with a vertical test section.

Phase Doppler Anemometry (PDA) was used to determine velocity profiles and turbulence intensity in the middle of the test section (Figure 2). Seeding particles with a diameter of approx. 1.5 μm were introduced in the suction of the fan and they followed the flow well due to their low Stokes number, thus providing results with a reasonable accuracy. The velocity profile and the intensity of the turbulence are shown in Figures 3 and 4. Counterflow velocities and turbulence intensities were measured in highlighted points in Figure 2 for three different fan velocities. The intensity of the turbulence was mostly around 2%, which can be considered a valid result.

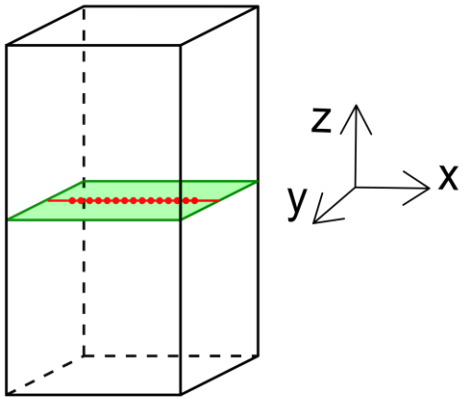

Fig. 2. Test section with with a highlighted cross-section.

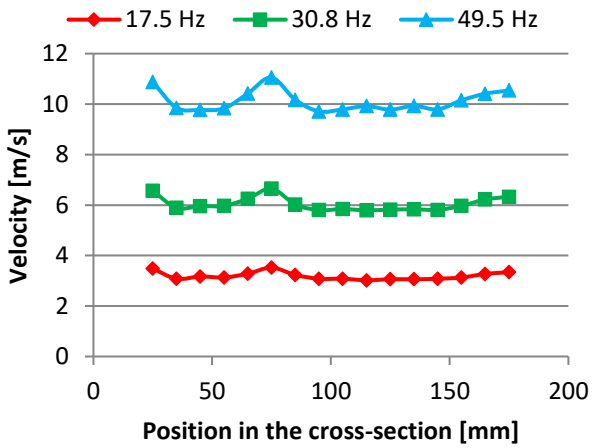

Fig. 3. Velocity profile of the test section measured in the middle of the cross-section.

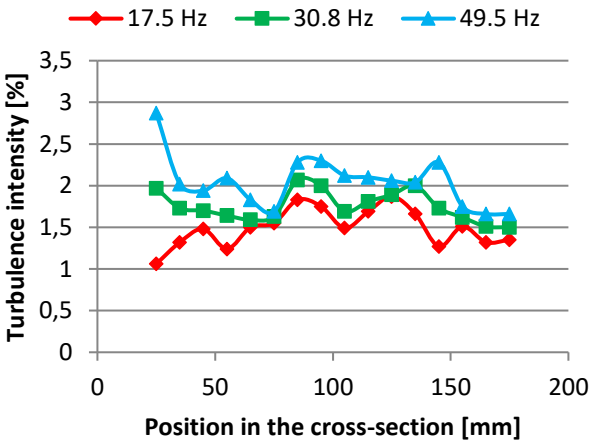

Fig. 4. Turbulence intensity.

2.2 Steel wire

The wires used in this study were taken from a knitted steel mesh, and therefore these wires were not straight. Both wires were attached in the corners of the test section (Figure 5). Due to the concave and convex shapes of the wires, there was a natural crossing on the axis of the test section. It was the same crossing as it is in the standard knitted wire mesh. The diameter of the wire was 0.8 mm and was made of AISI 304 stainless steel.

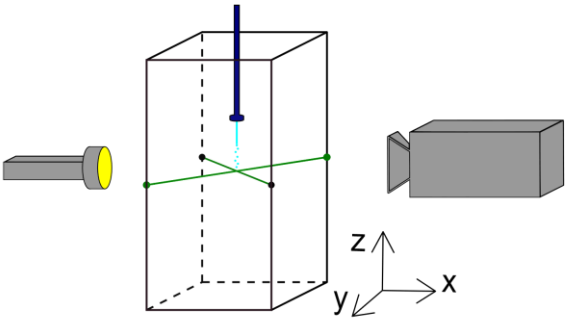

Fig. 5. Experimental setup.

2.3 Liquid

The working liquid was water at room temperature 20 °C. The liquid was pumped with a peripheral pump through a single orifice nozzle with a diameter of approximately 0.6 mm. This nozzle created a liquid jet. The orifice was placed 200 mm above the crossing. The liquid jet collapsed due to the Plateau-Rayleigh instability to droplets with diameters ranging from 0.8 to 1.2 mm. The following Table 1 shows the controlled input parameters i.e., the liquid flow rate and air flow velocity.

Table 1 Input parameters

Liquid flow rate [kg/h]			
3.8	8	12	
Air flow velocity [m/s]			
0	3	6	9

2.4 Camera and software

A high-speed camera Photron FASTCAM SA-Z type 2100K-M-16GB was used to capture images with a record rate of 20 000 fps. The shutter speed was 1.25 µs. The images were then processed with a MATLAB® code and the PIVlab add-on [19] to determine the velocity of the dispersed liquid. The angle of dispersed liquid and the atomization efficiency was analysed manually.

3 RESULTS AND DISCUSION

In the current study, three output parameters were monitored. The first one is the velocity of the dispersed liquid 12 mm downstream of the crossing. The second parameter is the angle at which the liquid is dispersed downstream of the crossing. The last one is the atomization rate determined by a qualitative description of the liquid dispersion.

The liquid flow rate was generalized by the Weber number We_d of the mother droplet before impact. This dimensionless number is defined in Equation 1:

$$We\_d = \frac{\rho \cdot u_d^2 \cdot D_o}{\sigma} \quad (1)$$

where ρ [kg/m^3] is the density of water, u_d [m/s] corresponds to the mean velocity of mother droplets, D_o [m] is the mean diameter of mother droplets and σ [mN/m] is the liquid surface tension of water.

The second dimensionless number is the relative velocity re_v defined in Equation 2 as a velocity of the dispersed liquid u_{liq} divided by the mean velocity of mother droplets u_d:

$$re\_v = \frac{u_{liq}}{u_d} \quad (2)$$

3.1 Velocity

The velocity component of the dispersed liquid in the direction of the axis -z was derived from a rectangle at the bottom of each image (Figure 6). Figure 6 displays the impact of the droplets with We_d = 2217 on the crossing of two wires with the zero velocity of the air counterflow.

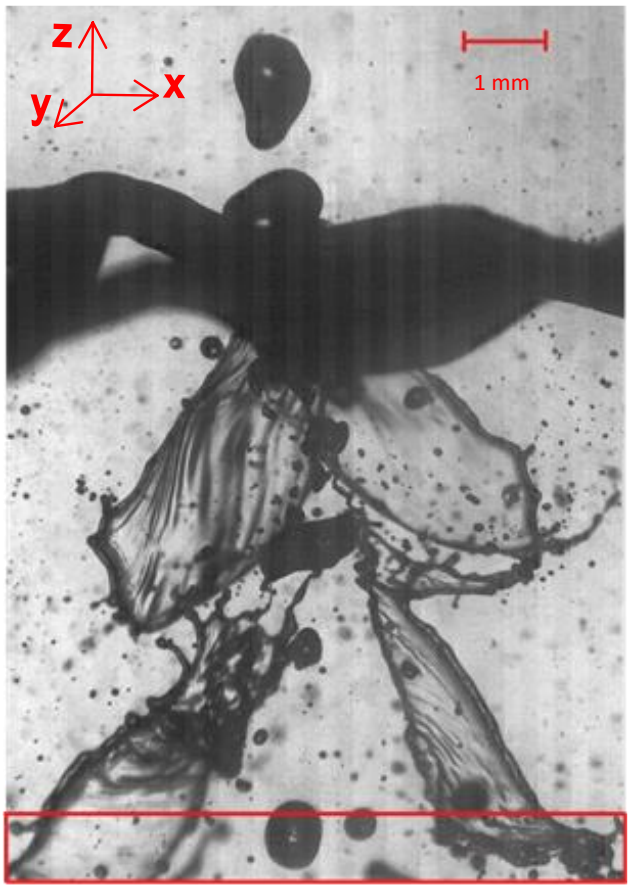

Fig. 6. The liquid dispersion on the crossing of two wires, We_d = 2217 and zero velocity of the air counterflow.

The velocity of mother droplets created from the jet before the impact was found to be approx. 3.5 m/s for the liquid flow rate of 3.8 kg/h. The velocity of droplets was 7.6 m/s for 8 kg/h, and the highest flow rate created droplets with the velocity of 12 m/s. Results can be seen in the Figure 7. The relative velocity of the dispersed liquid slows down with increasing velocity of the air counterflow but only for cases with We_d equal to 205 and 1073. For We_d = 2217, the relative velocity of the dispersed liquid increases. This phenomenon could be related to a feature of liquid jets. A liquid jet tends to drift with higher liquid flow rates and thus the stream of mother droplets created by the jet disintegration impacts on the crossing in various positions. Hence some droplets lost more kinetic energy than others which leads to differences in the velocity of dispersed liquid for We_d = 2217.

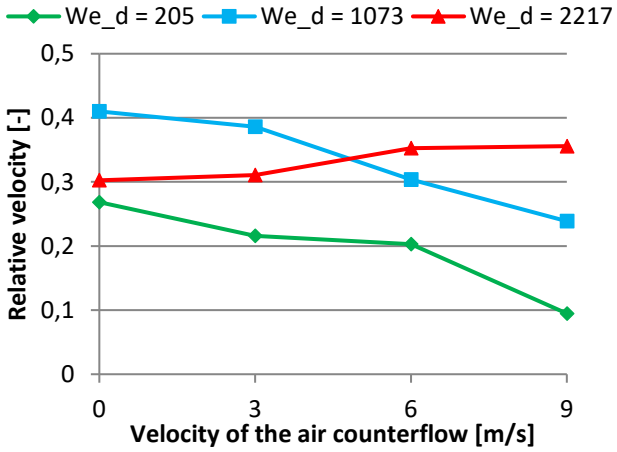

Fig. 7. Influence of the air velocity on the relative velocity of the dispersed liquid for different mother droplets' Weber numbers.

3.2 Angle

Figure 8 shows a method to determine the angle downstream the crossing. Overall results for the cone angle of the dispersed liquid can be seen in Figure 8. The angles were determined only for We_d equal to 1073 and 2217. For We_d = 205, the liquid generated only jets of

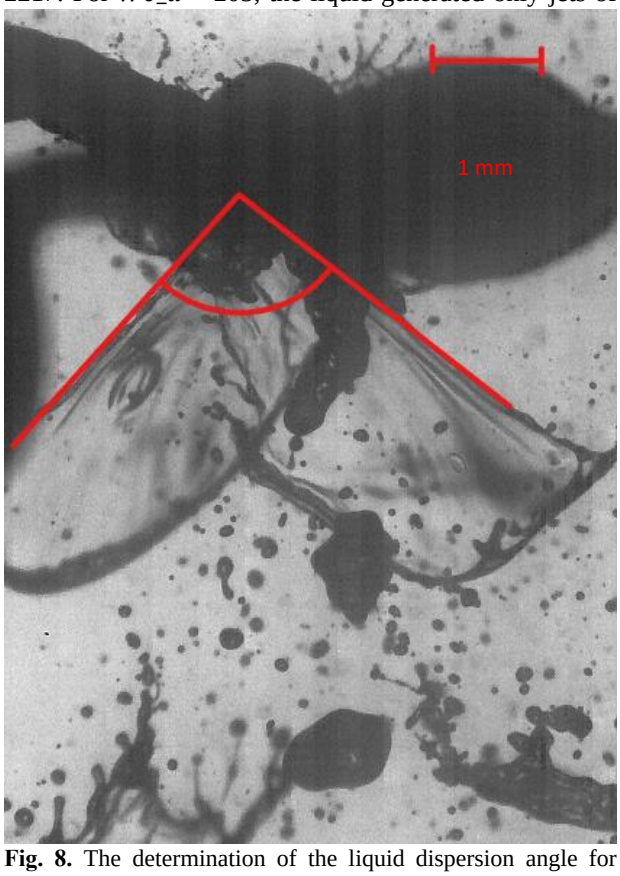

Fig. 8. The determination of the liquid dispersion angle for We_d = 2217 and counterflow velocity of 3 m/s.

Results in Figure 9 can be interpreted to mean that the air counterflow velocity has no influence on the cone angle. However, the liquid flow rate shows a significant impact on the cone angle. Therefore, the higher the liquid flow rate, the broader the cone angle. These results correspond with the research in [13].

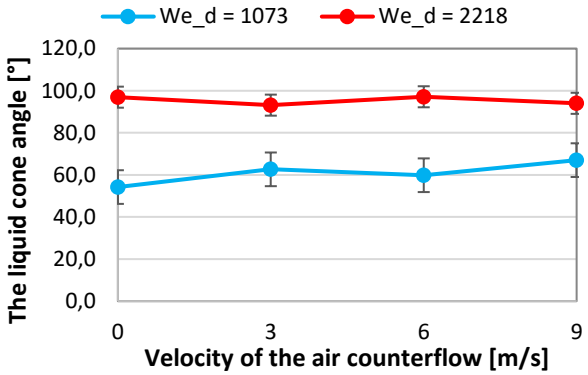

Fig. 9. Influence of the airflow velocity and mother droplets We_d on the cone angle of the liquid dispersion.

3.3 Dispersion

Atomization rate determined by a qualitative description of the liquid dispersion can be seen in Figures 10 (a), (b) and (c). Figure 10 (a) is for the lowest liquid flow rate defined by We_d = 205. This figure shows no liquid dispersion downstream the crossing. The liquid after the impact continues as a slow jet that will presumably disintegrate due to the Plateau-Rayleigh instability further downstream.

Figure 10 (b) shows mother droplets with We_d = 1073. Droplets in this mode disperse into liquid sheets with thick walls. These sheets quickly form jets.

The highest liquid flow rate with the Weber number of mother droplets We_d = 2218 forms more stable liquid sheets which disintegrate due to the Kelvin-Helmholtz instability (Figure 10 (c)). Dispersion for this We_d also presents the finest daughter droplets which arise from the dispersion of all observed input parameters. Similar conclusions were found in [14].

4 CONCLUSIONS

Research on the liquid dispersion on the crossing of two wires took place in the wind tunnel to determine the influence of the air counterflow rate on the liquid disintegration after the impact.

Velocity profiles and turbulence intensity in the wind tunnel were found to be reasonable for this study. Velocity component of the dispersed liquid in the direction of the axis -z, downstream the crossing, was evaluated with dimensionless numbers and important results are that the air counterflow velocity has a great impact on the liquid flow rates of 3.8 and 8 kg/h. Liquid flow rate of 12 kg/h shows some contrast to lower flow rates. This could be caused by the natural jet drifting. The next study will purposefully describe jet placed right above the crossing. Hence the influence of the drifting will be suppressed. The cone angle was described for liquid flow rates 8 and 12 kg/h and the conclusion is that the angle is only dependent on the liquid flow rate, not on the airflow velocity. The higher liquid flow rate has also an influence on the atomization rate since with a higher We_d dispersed mother droplets created a thinner wall of the liquid sheet.

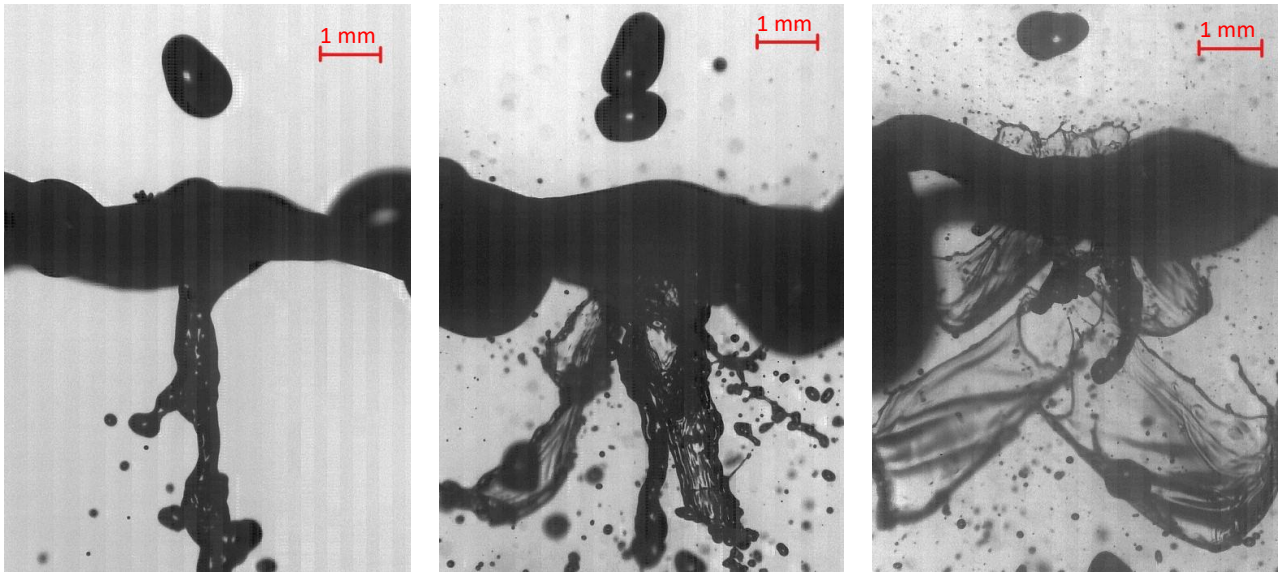

(a) (b) (c)

Fig. 10. Images of the liquid dispersion for different input parameters : (a) We_d = 205, the air flow velocity 0 m/s, (b)We_d = 1073, the air flow velocity 3 m/s, (c) We_d = 2218, the air flow velocity 6 m/s.

Thus, daughter droplets from the disintegration of the liquid sheet were smaller, and smaller droplets would create greater interface for the mass transfer. A problem that arises with small droplets is their predisposition to be blown off with the air counterflow. In industry, this means that potentially dangerous chemicals could be released to nature. Hence, it is a direction for the next research.

ACKNOWLEDGEMENTS

The authors acknowledge the financial support from the grant The effect of ambient airflow on the quality of liquid dispersion on the wire mesh, which is realised within the project Quality Internal Grants of BUT (KInG BUT), Reg. No. CZ.02.2.69/0.0/0.0/19_073/0016948, which is financed from the OP RDE. This work was supported by the project no. GA 21-45227L funded by the Czech Science Foundation and the project FSI-S-20-6295 funded by the Brno University of Technology.

LIST OF SYMBOLS

u_d	Mean velocity of droplets
ρ	Density
D_o	Mean diameter of droplets
σ	Liquid surface tension
We	Weber number
re_v	Relative velocity
u_{liq}	Velocity of dispersed liquid

REFERENCES

1. M. Maly, J. Jedelsky, J. Slama, L. Janackova, M. Sapik, G. Wigley, M. Jicha, Int. J. Heat Mass Transf. **123** 805 (2018)
2. M. Zaremba, J. Kozák, M. Malý, L. Weiß, Rudolf, J. Jedelský, M. Jícha, Int. J. Multiph. Flow **103** 1 (2018)
3. M. Hafezi, M. Mozaffarian, M. Jafarikojour, M. Mohseni, B. Dabir, Photochem. Photobiol. A 389 112198 (2020)
4. D. Tian, X. Zhang, X. Wang, J. Zhai, L. Jiang, Phys. Chem **13** 14606 (2011)
5. D. Soto, H.L. Girard, A. le Helloco, T. Binder, D. Quéré, K.K. Varanasi, Phys. Rev. Fluids **3** 1 (2018)
6. C. Ramshaw, R.H. Mallinson, US4283255A, 1981
7. Y. Luo, J.Z. Luo, G.W. Chu, Z.Q. Zhao, M. Arowo, J.F. Chen, Chem. Eng. Sci. **170** 347 (2017)
8. M.-J. Su, Y. Luo, G.-W. Chu, W. Liu, X.-H. Zheng, J.-F. Chen, Ind. Eng. Chem. Res **57** 4743 (2018)
9. G.E. Cortes Garcia, J. van der Schaaf, A.A. Kiss, J. Chem. Technol **92** 1136 (2017)
10. L. Sun, S. Lin, B. Pang, Y. Wang, E. Li, X. Zu, K. Zhang, X. Xiang, L. Chen, Phys. Fluids **33** (2021)
11. M.-J. Su, Y. Le, G.-W. Chu, Y.-B. Li, L.-L. Zhang, Y. Luo, Ind. Eng. Chem. Res **59** 3584 (2020)
12. J.P. Zhang, Y. Luo, G.W. Chu, L. Sang, Y. Liu, L.L. Zhang, J.F. Chen, Chem. Eng. Sci. **170** 204 (2017)
13. M.J. Su, Y. Luo, G.W. Chu, Y. Cai, Y. Le, L.L. Zhang, J.F. Chen, Chem. Eng. Sci **219** 115593 (2020)
14. Y.Y. Tang, M.J. Su, G.W. Chu, Y. Luo, Y.Y. Wang, L.L. Zhang, J.F. Chen, Chem. Eng. Sci. **198** 144 (2019)
15. L.F. Haim, I. Sher, E. Sher, ICLASS 2012 - 12th ICLASS (2012)
16. Y.Z. Lu, W. Liu, Y.C. Xu, Y. Luo, G.W. Chu, J.F. Chen, Chem. Eng. Process **140** 136 (2019)
17. Y. Wang, Y. bin Li, M.J. Su, G.W. Chu, B.C. Sun, Y. Luo, Chem. Eng. Sci. **240** 116675 (2021)
18. O. Cejpek, Design and realization of an aerodynamic tunnel for spraying nozzles, Diploma thesis (2020)
19. W. Thielicke, R. Sonntag, J. Open Res. Softw. **9** (2021)